

# Highly Sensitive Nonenzymatic Glucose Sensor Based on Reduced Graphene Oxide/Ultrasmall Pt Nanowire Nanocomposites

Xianming Fu<sup>1</sup>, Zhenming Chen<sup>2</sup>, Siyu Shen<sup>1</sup>, Lilan Xu<sup>1</sup>, Zhimin Luo<sup>3,\*</sup>

<sup>1</sup> School of Pharmacy and Medical Technology, Putian University, Xueyuan Middle Street 1133#, Putian 351100, China

<sup>2</sup> Guangxi Key Laboratory of Calcium Carbonate Resources Comprehensive Utilization, College of Materials & Environmental Engineering, Hezhou University, Xihuan Road 18#, Hezhou 542899, China

<sup>3</sup> Key Laboratory for Organic Electronics & Information Displays and Institute of Advanced Materials (IAM), Nanjing University of Posts and Telecommunications, Wenyuan Road 9#, Yadong New District, Nanjing 210023, China

\*E-mail: [iamzmluo@hotmail.com](mailto:iamzmluo@hotmail.com)

Received: 22 January 2018 / Accepted: 2 March 2018 / Published: 10 April 2018

---

An amperometric nonenzymatic biosensor for sensitive and selective detection of glucose has been developed by using reduced graphene oxide/ultrasmall platinum nanowire nanocomposites (rGO-PtNW) as electrode material. rGO-PtNW displays good electrocatalytic activity towards the oxidation of glucose in alkaline solution. The fabricated biosensor shows good analytical performance including low detection limit (4.6  $\mu\text{mol/L}$ ), wide linear range (0.032-1.89 mmol/L), high sensitivity (56.11  $\mu\text{A}\cdot(\text{mmol/L})^{-1}\cdot\text{cm}^{-2}$ ), and good anti-interfering ability towards species (uric acid and ascorbic acid) coexisting with glucose in human blood at the work potential of 0 V. It indicated that rGO-PtNW nanocomposite can serve as a promising candidate material for high-performance glucose nonenzymatic biosensors.

---

**Keywords:** glucose; biosensor; nonenzymatic sensor; reduced graphene oxide; Pt nanowire

## 1. INTRODUCTION

Diabetes mellitus is a kind of metabolic diseases caused by the defect of insulin secretion or the damage of its biological function. Nowadays, diabetes mellitus has become a serious public health problem and the number with adult diabetes continues to rise. Diabetes mellitus often brings some complications, such as diabetic neuropathy, renal failure, diabetic foot and blindness [1], which

seriously affect people's health and quality of life. So the accurate and rapid detection of human's blood glucose level is of extraordinary significance for the early diagnosis and treatment of diabetes. At present, numerous commercial glucose biosensors are available for diabetic patients, in which electrochemical biosensor plays a leading role due to its simplicity, reliability and cheapness [2]. Electrochemical sensors for glucose detection include glucose oxidase (GOx) and nonenzymatic glucose (NEG) sensor. GOx as enzymatic catalyst has been widely used for fabricating glucose biosensor [3-5]. Although good selectivity and high sensitivity have been achieved, this kind of enzymatic sensor still has some inevitable defects, including the complexity of enzyme immobilization, and the easy inactivation and degeneration of enzyme [6]. Direct electrocatalytic oxidation of glucose carried out on an enzyme-free electrode would avoid the drawbacks of the enzyme electrode. Therefore, NEG sensors have attracted great attention and various types of NEG sensors have been developed in recent years [6-10].

Nanomaterials have been extensively applied in sensors owing to their interesting electrochemical properties in the past few years [11-15]. Transition metal nanoparticles, especially noble metal nanoparticles modified electrode surfaces, exhibit high catalytic activity for many electrochemical reactions, which promotes the creativity and development of various electrochemical sensors [16]. In particular, Pt nanomaterials played an important role in the application of biosensors. Pt or Pt-based alloy electrocatalysts were widely used for nonenzymatic detection of glucose [17-19]. Effort to enhance the catalytic activity of Pt has concentrated on the dispersion of nanoparticles onto carbon-based supporting materials with high surface area, such as highly ordered mesoporous carbon [20], carbon nanofiber [21], carbon nanotube [22,23], etc.

Recently, a new allotrope of carbon material, graphene, has attracted extensive attention. Graphene is a single layer of carbon atoms closely packed into a honeycomb two-dimensional lattice. Owing to its unique physical and chemical properties, such as extremely high specific surface area [24,25], excellent electric conductivity [26,27], ease of functionalization and production [28,29], graphene, including graphene oxide (GO) or reduced graphene oxide (rGO), has been used as an ideal platform for the preparation and stabilization of Au [30], Ag [31], Pt [32] and Pd [33] nanoparticles with many potential applications.

In this article, reduced graphene oxide/ultrasmall Pt nanowire nanocomposite (rGO-PtNW) was synthesized by a simple one-pot wet-chemical method and used to modify glassy carbon electrode (GCE) for fabricating a novel nonenzymatic glucose biosensor. The electrochemical behavior of this biosensor has been investigated by cyclic voltammetry (CV) and amperometric methods. Due to the synergy effect of rGO and PtNW, the resultant nonenzymatic biosensor based on rGO-PtNW demonstrates good analytical performance for detecting glucose.

## 2. MATERIALS AND METHODS

### 2.1. Reagents and apparatus

Graphite, uric acid (UA), ascorbic acid (AA) and Nafion were purchased from Sigma-Aldrich. Chloroplatinate acid ( $\text{H}_2\text{PtCl}_6 \cdot 6\text{H}_2\text{O}$ ) was obtained from Shanghai Chemical Reagent Company. D-glucose was provided by Beijing Chemical Reagent Company. Potassium permanganate ( $\text{KMnO}_4$ ,

99%) and concentrated sulfuric acid ( $\text{H}_2\text{SO}_4$ , 98%) were supplied by Aladdin Reagent Co., Ltd. All other chemicals were analytical grade and used as received. Aqueous solutions were prepared with deionized water (18.2 M $\Omega$  cm) from a Millipore system.

Transmission electron microscopy (TEM) and high-resolution transmission electron microscopy (HRTEM) images of as-synthesized nanocomposites were recorded on a JEM-2011F electron microscope (JEOL, Japan). Raman spectra of nanocomposites were measured using a reflex Raman micro-spectrometer (Renishaw INVIA, Britain). All electrochemical measurements were performed using a CHI 660D Electrochemical Workstation (CH Instruments, China) and a conventional three-electrode system with an Ag/AgCl (3 mol/L KCl) reference electrode, a platinum wire counter electrode, and a glassy carbon working electrode (GCE, 3 mm in diameter).

## 2.2. Synthesis of rGO-PtNW

Graphite oxide was prepared from natural graphite powder by a modification of Hummers' and Offeman's method [3]. The formation of rGO-PtNW nanocomposites was achieved by the simultaneous catalytic reduction of GO and  $\text{H}_2\text{PtCl}_6$  with HCOOH. GO aqueous suspension (0.8 mg/mL, 1.0 mL) and  $\text{H}_2\text{PtCl}_6 \cdot 6\text{H}_2\text{O}$  solution (10.0 mg/mL, 0.25 mL) and HCOOH (0.3 mL) were added together into a flask. After 30 min of ultrasonic treatment, the mixture was placed in a closed vessel to allow the reaction continued at room temperature without stirring for two days. When the growth of PtNW and the synchronous catalytic reduction of GO were completed, the product was centrifuged for 15 min at 5000 rpm, and then washed with deionized water and ethanol, respectively. Finally, the product was dried overnight in a 60 °C vacuum drying oven.

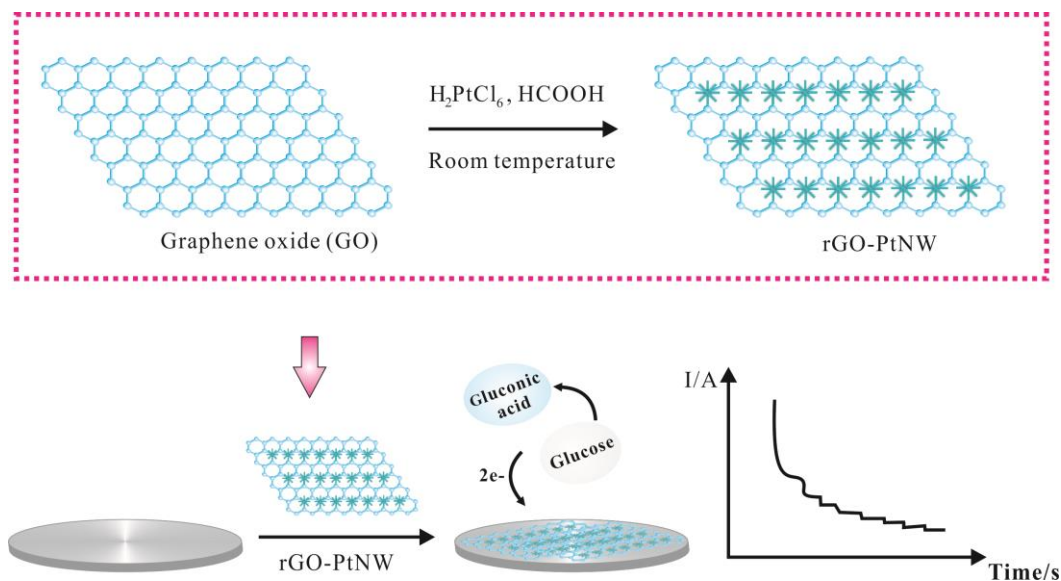
## 2.3. Sensor fabrication and electrochemical measurements

GCE was carefully polished with 0.3 and 0.05  $\mu\text{m}$  alumina powder to obtain a mirror-shiny surface, and then thoroughly rinsed with deionized water and ethanol for 1 min under sonication. The rGO-PtNW nanocomposites were first dispersed in the mixed solvent of ethanol and  $\text{H}_2\text{O}$  (v:v=1:1), and a 30 min ultrasound was carried out to form a uniform rGO-PtNW suspension (1 mg/mL). Then 5.0  $\mu\text{L}$  of well-dispersive suspension was dripped onto the surface of polished GCE. After rGO-PtNW modified GCE was dried at room temperature, 5.0  $\mu\text{L}$  of 0.05 wt% Nafion was spread on the surface of the rGO-PtNW modified GCE to form a thin protective film.

Cyclic voltammetry (CV) curves of GCE and rGO-PtNW modified GCE in  $\text{N}_2$ -saturated 0.5 mol/L  $\text{H}_2\text{SO}_4$  aqueous solution were recorded in the potential ranging from -0.2 to 0.6 V at scan rate of 100 mV/s. CV curves of rGO-PtNW modified GCE in  $\text{N}_2$ -saturated 0.1 mol/L NaOH aqueous solution containing different concentration of glucose were recorded in the potential ranging from -1.0 to 0.6 V at scan rate of 50 mV/s. Amperometric experiments were carried out with successive adding glucose solution every 30 s at an applied potential of 0 V.

### 3. RESULTS AND DISCUSSION

#### 3.1. Experimental principle of the sensor based on rGO-PtNW



**Scheme 1.** Schematic presentation of rGO-PtNW modified GCE for nonenzymatic detecting glucose.

The principle of using rGO-PtNW to construct an enzyme free glucose sensor was illustrated in Scheme 1. rGO-PtNW was synthesized by the simultaneous chemical reduction of GO and  $\text{H}_2\text{PtCl}_6$  with  $\text{HCOOH}$ . Then rGO-PtNW was used to modify GCE for fabricating a nonenzymatic glucose biosensor. Glucose was electrochemically oxidized to gluconic acid on the surface of modified GCE in alkaline solution, and the response current during the reaction was detected, which provided the basis for the detection of glucose.

#### 3.2. Characterization of the prepared rGO-PtNW

The morphology of rGO nanosheets was characterized by TEM and HRTEM. Fig. 1a shows that rGO nanosheets appear as a transparent and slightly wrinkled sheet. The interlayer spacing of rGO nanosheets is about 0.343 nm (Fig. 1b), which corresponds to the spacing of graphene layers. Fig. 1c presents the successful growth of ultrasmall platinum nanowires on the surface of graphene nanosheets. They are clustered into small clusters and dispersed on the nanosheets. The length of the Pt nanowires is about 4-10 nm and the diameter is about 2-3 nm (Fig. 1d). The inset in Fig. 1d is the crystal lattice of this Pt nanowire, revealing the entire nanowire is one single crystal and the interplanar spacing is 0.194 nm, which is consistent with the value of most Pt crystals [34,35]. Fig. 2 shows the Raman spectrum of rGO-PtNW. G band at  $1580\text{ cm}^{-1}$  and D band at  $1345\text{ cm}^{-1}$  ascribed to graphene indicate the structure of graphene in rGO-PtNW.

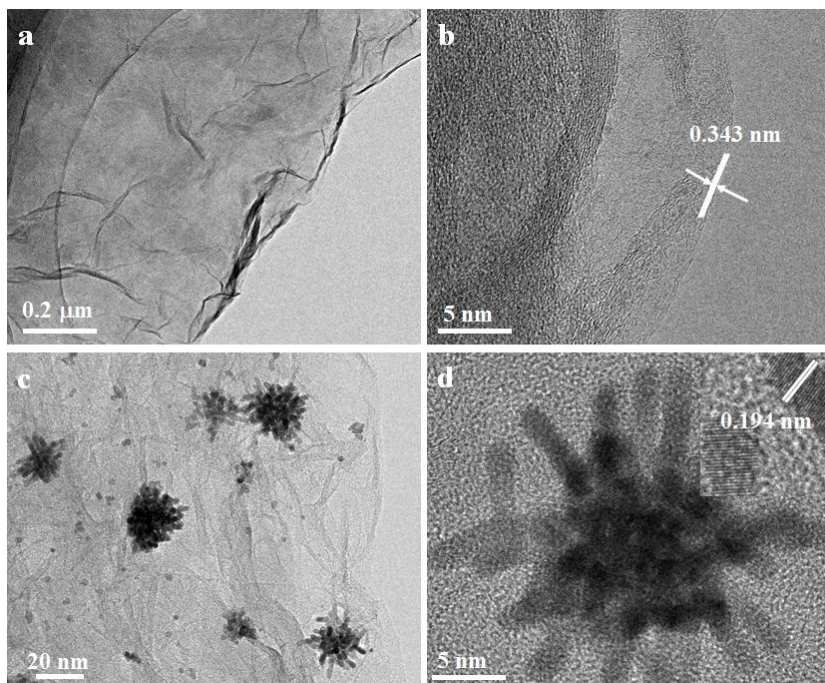


**Figure 1.** (a) TEM and (b) HRTEM images of rGO nanosheets. (c) TEM and (d) HRTEM images of ultrasmall Pt nanowires on rGO nanosheets. Inset in d is the magnified HRTEM image of crystal lattice of an ultrasmall Pt nanowire on rGO nanosheets.

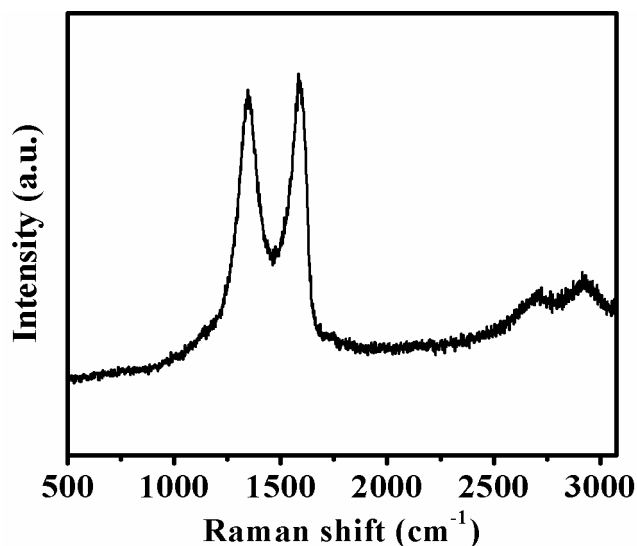


**Figure 2.** Raman spectrum of rGO-PtNW.

### 3.3. Electrochemical measurements of rGO-PtNW/GCE

Fig. 3a shows the typical CV curves of the bare GCE and rGO-PtNW modified GCE in  $N_2$ -saturated 0.5 mol/L  $H_2SO_4$  aqueous solution. No oxidation or reduction peak is observed at bare GCE. rGO-PtNW/GCE shows peaks ranging from -0.2 to 0.2 V, which are ascribed to hydrogen absorption and desorption of PtNW in acidic solution [34]. In order to measure the response of rGO-PtNW modified GCE to glucose, CVs of rGO-PtNW/GCE were conducted in  $N_2$ -saturated 0.1 mol/L NaOH

solution in the absence and presence of glucose, respectively. As shown in Fig. 3b, only a small background current is observed at the rGO-PtNW/GCE in 0.1 mol/L NaOH aqueous solution. After glucose was added into NaOH aqueous solution, the current signal corresponding to electrochemical oxidation and reduction of glucose increases with the increase of glucose concentration, which provides the basis for quantitative detection of glucose.

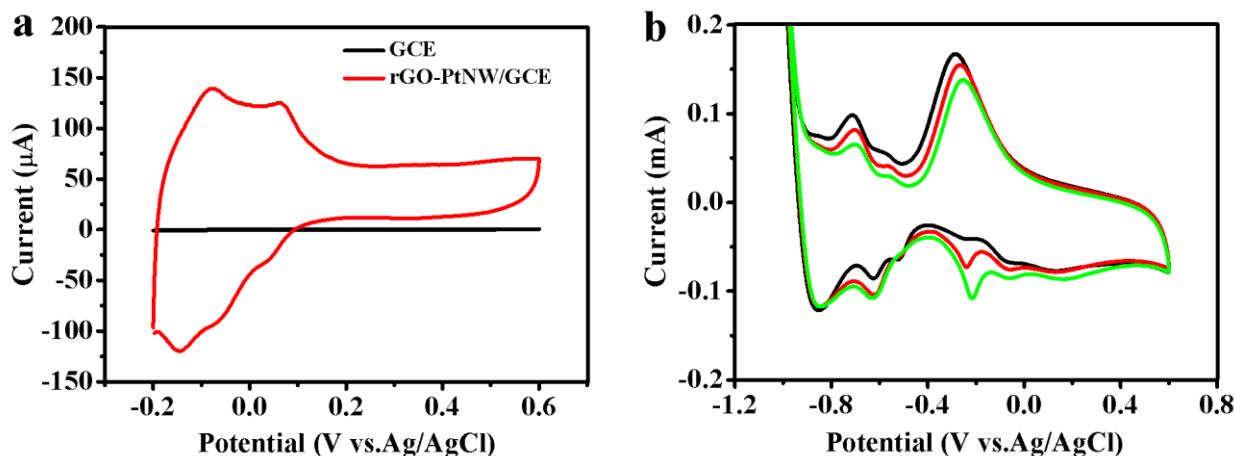


**Figure 3.** (a) CV curves of GCE (black), rGO-PtNW modified GCE (red) in N<sub>2</sub>-saturated 0.5 mol/L H<sub>2</sub>SO<sub>4</sub> aqueous solution at scan rate of 100 mV/s. (b) CV curves of rGO-PtNW modified GCE in N<sub>2</sub>-saturated 0.1 mol/L NaOH aqueous solution in the absence (black) and presence of 1.96 mmol/L glucose (red), 7.41 mmol/L glucose (green) at scan rate of 50 mV/s.

### 3.4. The sensitivity of the sensor

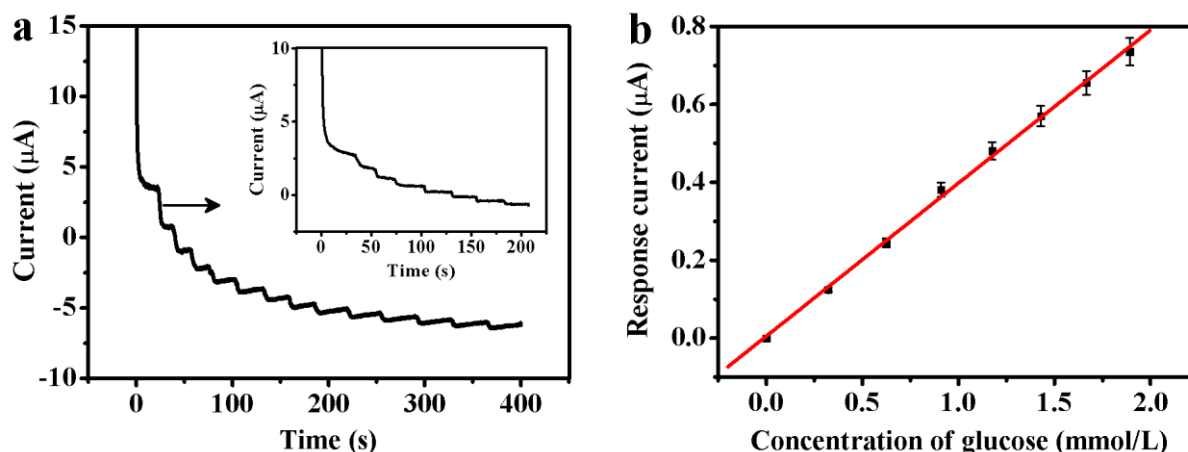


**Figure 4.** (a) Amperometric response of the rGO-PtNW modified GCE to successive addition of 100 μL of 100 mmol/L glucose and 10 μL of 10 mmol/L glucose (inset) into 5 mL of 0.1 mol/L NaOH aqueous solution at an applied potential of 0 V. (b) Calibration curve of response currents versus concentrations of added glucose.

Amperometric technique was used to evaluate the detection of glucose by rGO-PtNW-based biosensor. Fig. 4a shows the typical amperometric response of rGO-PtNW/GCE to successive

additions of 100  $\mu\text{L}$  of 100 mmol/L glucose and 10  $\mu\text{L}$  of 10 mmol/L glucose into 0.1 mol/L NaOH aqueous solutions with an applied potential of 0 V. It should be noted that 0 V was chosen as the detection potential since such a low potential would be beneficial for reducing the background current and minimizing the responses of general interfering species. The biosensor based on rGO-PtNW reaches steady-state current after the addition of glucose within 7 s, indicating its fast and sensitive response toward glucose. Fig. 4b displays the calibration curve of the response current and the glucose concentration. The biosensor exhibits a fine linear relationship with the concentration of glucose in the range of 0.032-1.89 mmol/L ( $R = 0.999$ ). The detection limit is calculated to be 4.6  $\mu\text{mol/L}$  based on  $S/N = 3$  and the sensitivity of the as-prepared biosensor is calculated to be  $56.11 \mu\text{A} \cdot (\text{mmol/L})^{-1} \cdot \text{cm}^{-2}$ . The performance of the biosensor was compared with the previously reported nonenzymatic glucose sensors. As shown in Table 1, the presented biosensor has a lower detection limit, indicating that the GCE modified with rGO-PtNW exhibits good affinity to glucose. High sensitivity of this biosensor may be attributed to a large surface area, a fast electron transfer activity of rGO-PtNW [36-38], and the synergetic electrocatalytic effect of PtNW and graphene towards glucose [39-41].

**Table 1.** Performance comparison of nonenzymatic glucose biosensors based on electrodes modified with different materials.

Materials	Detection potential (V)	Sensitivity ( $\mu\text{A} \cdot (\text{mmol/L})^{-1} \cdot \text{cm}^{-2}$ )	Linear range (mmol/L)	Detection limit ( $\mu\text{mol/L}$ )	Reference
PtPd/MCV	-0.02	0.11	1.5-12	120	[7]
CNT-PtNP	-0.4	-	0.028-46.6	28	[22]
Pt/OMCs	-0.08	16.69	0.5-4.5	130	[42]
PtRu-MWNT-IL	-0.1	10.7	0.2-15	50	[43]
NPGF	-0.15	232	1-14	53.2	[44]
PG/OPPyNF/CoPcTS	-	5.695	0.25-20	100	[45]
Pt-PbNAE	-0.2	11.25	0.008-11	8	[46]
rGO-PtNW	0	56.11	0.032-1.89	4.6	This work

### 3.5. The selectivity of the sensor

As we all know, there are some easily oxidative species such as uric acid (UA), ascorbic acid (AA) and other carbohydrate compounds usually co-exist with glucose in human blood. Although the normal physiological levels of UA (0.02 mmol/L) and AA (0.1 mmol/L) are lower than that of glucose (3-8 mmol/L), they have higher electron transfer rates than glucose, which leads to their oxidation currents comparable to that of highly concentrated glucose. The lower operation potential may greatly minimize the interference from easily oxidative compounds in the procedure of detecting glucose. The effects of UA and AA upon the response of the glucose biosensor were evaluated at working potential of 0 V. As seen from Fig. 5, the addition of 0.02 mmol/L UA and 0.1 mmol/L AA into 1.0 mmol/L

glucose solution caused only little effect on the response of the glucose. Interference from coexisting compounds is negligible, which shows that the biosensor has a good anti-interfering ability.

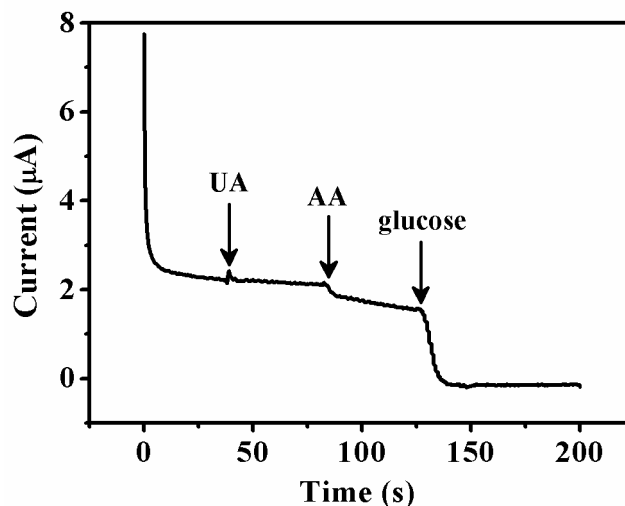


**Figure 5.** Amperometric response of the rGO-PtNW/GCE to 0.02 mmol/L UA, 0.1 mmol/L AA, 1.0 mmol/L glucose at 0 V in 0.1 mol/L NaOH aqueous solution.

The reproducibility and stability of this glucose biosensor were also estimated. Six rGO-PtNW modified electrodes prepared in the same manner produced a RSD (the relative standard deviation) of 4.76% in current response to 0.5 mmol/L glucose, indicating an acceptable reproducibility. The response current almost remained unchanged after the electrode was stored under room temperature for 20 days, demonstrating a long-term storage stability of the electrode.

### 3.6. Real sample analysis

**Table 2.** Glucose content determination in human plasma samples.

Sample number	Glucose concentration provided by the affiliated hospital of Putian University (mmol/L)	Glucose concentration determined by the proposed biosensor (average of 3 times) (mmol/L)	Relative error (%)
1	4.27	4.34 ± 0.18	+1.64
2	4.96	5.06 ± 0.24	+2.02
3	5.48	5.26 ± 0.26	-4.01
4	6.24	6.02 ± 0.32	-3.53
5	8.62	8.91 ± 0.46	+3.36

The feasibility of the proposed biosensor in practical analysis was evaluated by determining the glucose in human plasma samples. Fresh plasma samples were provided by the affiliated hospital of Putian University and the donors all informed consent. Five plasma samples were firstly tested in the

affiliated hospital with Roche Cobas 8000 analyzer. Then the samples were assayed with the biosensor. The response current was obtained at 0 V with the addition of 100  $\mu\text{L}$  of sample into 5 mL of 0.1 mol/L NaOH solution and the contents of glucose in blood can be calculated from the calibration curve. As show in Table 2, the results obtained from this biosensor are in agreement with those provided by the hospital.

#### 4. CONCLUSIONS

In summary, rGO-PtNW was synthesized by a facile one-pot wet-chemical approach to develop a nonenzymatic glucose biosensor. The rGO-PtNW modified GCE displays high electrocatalytic activity towards the oxidation of glucose, showing satisfactory analytical performance with a wide linear range from 0.032 to 1.89 mmol/L, low detection limit (4.6  $\mu\text{mol/L}$ ) and high sensitivity (56.11  $\mu\text{A}\cdot(\text{mmol/L})^{-1}\cdot\text{cm}^{-2}$ ). Meanwhile, the interference from the oxidation of some interfering species such as UA and AA is effectively avoided. All these characteristics suggest that the rGO-PtNW holds a good promise for the development of nonenzymatic glucose biosensor.

#### ACKNOWLEDGEMENTS

This work was financially supported by the Education and Scientific Research Project of Middle-aged and Young Teachers in Fujian Province (JAT170512), the Scientific Research Project of Putian University (2016042), the Doctor's Scientific Research Foundation of Hezhou University (HZUJS201512) and the Infrastructure Upgrading Project of Guangxi College Middle-aged and Young Teachers (KY2016YB458).

#### References

1. X.Y. Jiang, Y.H. Wu, X.Y. Mao, X.J. Cui and L.D. Zhu, *Sens. Actuators B: Chem.*, 153 (2011) 158.
2. J. Li, H.F. Hu, H.Y. Li and C.B. Yao, *J. Mater. Sci.*, 52 (2017) 10455.
3. Z.M. Luo, X.B. Ma, D.L. Yang, L.H. Yuwen, X.R. Zhu, L.X. Weng and L.H. Wang, *Carbon*, 57 (2013) 470.
4. Z.M. Luo, L.H. Yuwen, Y.J. Han, J. Tian, X.R. Zhu, L.X. Weng and L.H. Wang, *Biosens. Bioelectron.*, 36 (2012) 179.
5. P. Wu, Q. Shao, Y.J. Hu, J. Jin, Y.J. Yin, H. Zhang and C.X. Cai, *Electrochim. Acta*, 55 (2010) 8606.
6. L.C. Jiang and W.D. Zhang, *Biosens. Bioelectron.*, 25 (2010) 1402.
7. X.J. Bo, J. Bai, L. Yang and L.P. Guo, *Sens. Actuators B: Chem.*, 157 (2011) 662.
8. X. Wang, C.G. Hu, H. Liu, G.J. Du, X.S. He and Y. Xi, *Sens. Actuators B: Chem.*, 144 (2010) 220.
9. X.L. Chen, H.B. Pan, H.F. Liu and M. Du, *Electrochim. Acta*, 56 (2010) 636.
10. H. Zhu, X.Q. Lu, M.X. Li, Y.H. Shao and Z.W. Zhu, *Talanta*, 79 (2009) 1446.
11. Z.H. Xu, C. He, T. Sun and L. Wang, *Electroanalysis*, 25 (2013) 2339.
12. Q. Wang, Y. Song, Y.Q. Chai, G.Q. Pan, T. Li, Y.L. Yuan and R. Yuan, *Biosens. Bioelectron.*, 60 (2014) 118.

13. R.M. Aran-Ais, F.J. Vidal-Iglesias, J. Solla-Gullon, E. Herrero and J.M. Feliu, *Electroanalysis*, 27 (2015) 945.
14. X.M. Fu, Z.J. Liu, S.X. Cai, Y.P. Zhao, D.Z. Wu, C.Y. Li and J.H. Chen, *Chin. Chem. Lett.*, 27 (2016) 920.
15. M.Wang, Z.X. Zheng, J.J. Liu and C.M. Wang, *Electroanalysis*, 29 (2017) 1258.
16. X. Chu, D.X. Duan, G.L. Shen and R.Q. Yu, *Talanta*, 71 (2007) 2040.
17. Y. Song, C.Z. Zhu, H. Li, D. Du and Y.H. Lin, *RSC Adv.*, 100 (2015) 82617.
18. L.Q. Rong, C. Yang, Q.Y. Qian and X.H. Xia, *Talanta*, 72 (2007) 819.
19. J. Ryu, K. Kim, H.S. Kim, H.T. Hahn and D. Lashmore, *Biosens. Bioelectron.*, 26 (2010) 602.
20. C. Su, C. Zhang, G.Q. Lu and C.A. Ma, *Electroanalysis*, 22 (2010) 1901.
21. V. Vamvakaki, K. Tsagaraki and N. Chaniotakis, *Anal. Chem.*, 78 (2006) 5538.
22. G. Wei, F.G. Xu, Z. Li and K.D. Jandt, *J. Phys. Chem. C*, 115 (2011) 11453.
23. S. Badhulika, R.K. Paul, Rajesh, T. Terse and A. Mulchandani, *Electroanalysis*, 26 (2014) 103.
24. D. Li, M.B. Muller, S. Gilje, R.B. Kaner and G.G. Wallace, *Nat. Nanotechnol.*, 3 (2008) 101.
25. Y.S. Bai, G.X. Sun, S. Chen, L.D. Lu and J.C. Bao, *Int. J. Electrochem. Sci.*, 12 (2017) 652.
26. A.K. Geim and K.S. Novoselov, *Nat. Mater.*, 6 (2007) 183.
27. K. Movlaee, M.R. Ganjali, M. Aghazadeh, H. Beitollahi, M. Hosseini, S. Shahabi and P. Norouzi, *Int. J. Electrochem. Sci.*, 12 (2017) 305.
28. Y. Wang, Y.Y. Shao, D.W. Matson, J.H. Li and Y.H. Lin, *ACS Nano*, 4 (2010) 1790.
29. W.R. Yang, K.R. Ratinac, S.P. Ringer, P. Thordarson, J.J. Gooding and F. Braet, *Angew. Chem. Int. Ed.*, 49 (2010) 2114.
30. X. Huang, X.Z. Zhou, S.X. Wu, Y.Y. Wei, X.Y. Qi, J. Zhang, F. Boey and H. Zhang, *Small*, 6 (2010) 513.
31. R. Pasricha, S. Gupta and A.K. Srivastava, *Small*, 5 (2009) 2253.
32. E. Yoo, T. Okata, T. Akita, M. Kohyama, J. Nakamura and I. Honma, *Nano Lett.*, 9 (2009) 2255.
33. X.M. Chen, G.H. Wu, J.M. Chen, X. Chen, Z.X. Xie and X.R. Wang, *J. Am. Chem. Soc.*, 133 (2011) 3693.
34. Z.M. Luo, L.H. Yuwen, B.Q. Bao, J. Tian, X.R. Zhu, L.X. Weng and L.H. Wang, *J. Mater. Chem.*, 22 (2012) 7791.
35. Y.J. Song, R.M. Garcia, R.M. Dorin, H.R. Wang, Y. Qiu, E.N. Coker, W.A. Steen, J.E. Miller and J.A. Shelnutt, *Nano Lett.*, 7 (2007) 3650.
36. F.G. Xu, Y.J. Sun, Y. Zhang, Y. Shi, Z.W. Wen and Z. Li, *Electrochem. Commun.*, 13 (2011) 1131.
37. S.J. Guo, D. Wen, Y.M. Zhai, S.J. Dong and E.K. Wang, *ACS Nano*, 4 (2010) 3959.
38. C.L. Sun, H.H. Lee, J.M. Yang and C.C. Wu, *Biosens. Bioelectron.*, 26 (2011) 3450.
39. H. Wu, J. Wang, X.H. Kang, C.M. Wang, D.H. Wang, J. Liu, I.A. Aksay and Y.H. Lin, *Talanta* 80 (2009) 403.
40. R.S. Dey and C.R. Raj, *J. Phys. Chem. C*, 114 (2010) 21427.
41. X.M. Feng, R.M. Li, C.H. Hu and W.H. Hou, *J. Electroanal. Chem.*, 657 (2011) 28.
42. X.J. Bo, J.C. Ndamanisha, J. Bai and L.P. Guo, *Talanta*, 82 (2010) 85.
43. F. Xiao, F.Q. Zhao, D.P. Mei, Z.R. Mo and B.Z. Zeng, *Biosens. Bioelectron.*, 24 (2009) 3481.
44. Y. Xia, W. Huang, J.F. Zheng, Z.J. Niu and Z.L. Li, *Biosens. Bioelectron.*, 26 (2011) 3555.
45. L. Ozcan, Y. Sahin and H. Turk, *Biosens. Bioelectron.*, 24 (2008) 512.
46. Y. Bai, Y.Y. Sun and C.Q. Sun, *Biosens. Bioelectron.*, 24 (2008) 579.